Gating of the Bacterial Sodium Channel, NaChBac: Voltage-dependent Charge Movement and Gating Currents

Alexey Kuzmenkin,[1] Francisco Bezanilla,[1,2,3] and Ana M. Correa[1]

[1]Department of Anesthesiology and [2]Department of Physiology, David Geffen School of Medicine at University of California, Los Angeles, Los Angeles, CA 90095

[3]Centro de Estudios Científicos, Valdivia, Chile

ABSTRACT The bacterial sodium channel, NaChBac, from *Bacillus halodurans* provides an excellent model to study structure–function relationships of voltage-gated ion channels. It can be expressed in mammalian cells for functional studies as well as in bacterial cultures as starting material for protein purification for fine biochemical and biophysical studies. Macroscopic functional properties of NaChBac have been described previously (Ren, D., B. Navarro, H. Xu, L. Yue, Q. Shi, and D.E. Clapham. 2001. *Science.* 294:2372–2375). In this study, we report gating current properties of NaChBac expressed in COS-1 cells. Upon depolarization of the membrane, gating currents appeared as upward inflections preceding the ionic currents. Gating currents were detectable at −90 mV while holding at −150 mV. Charge–voltage (Q–V) curves showed sigmoidal dependence on voltage with gating charge saturating at −10 mV. Charge movement was shifted by −22 mV relative to the conductance–voltage curve, indicating the presence of more than one closed state. Consistent with this was the Cole-Moore shift of 533 μs observed for a change in preconditioning voltage from −160 to −80 mV. The total gating charge was estimated to be 16 elementary charges per channel. Charge immobilization caused by prolonged depolarization was also observed; Q–V curves were shifted by approximately −60 mV to hyperpolarized potentials when cells were held at 0 mV. The kinetic properties of NaChBac were simulated by simultaneous fit of sodium currents at various voltages to a sequential kinetic model. Gating current kinetics predicted from ionic current experiments resembled the experimental data, indicating that gating currents are coupled to activation of NaChBac and confirming the assertion that this channel undergoes several transitions between closed states before channel opening. The results indicate that NaChBac has several closed states with voltage-dependent transitions between them realized by translocation of gating charge that causes activation of the channel.

KEY WORDS: sodium channel • gating charge • bacterial channels • C-type inactivation • Cole-Moore shift

INTRODUCTION

Voltage-gated ion channels are specialized proteins embedded in the cell membrane whose function is controlled by the electrical potential gradient across the membrane and that posses ion-conducting pores that are selective to a particular ion. Despite differences in their physiological functions, the general channel structure and the gating mechanisms show high evolutionary conservation among different channels that allows inferences on structure–function relationships from one channel type to the next. A new group of voltage-gated ion channels is emerging from the analysis of bacteria genomes. Recently, a voltage-gated Na^+ channel has been reported (Ren et al., 2001), the NaChBac obtained from *Bacillus halodurans*. Intriguingly, this channel reveals structural and functional features different from all other voltage-gated Na^+ channels described. First, it is built of only one domain containing six transmembrane segments connected by extra- and intracellular loops. Thus, it resembles the structure of most voltage-gated K^+ channels, rather than that of voltage-gated Na^+ or Ca^{2+} channels where a large pore-forming α-subunit consists of four six-transmembrane pseudodomains. Similar to K^+ channels, NaChBac monomers presumably assemble as tetramers to form functional channels. Second, despite its high selectivity to Na^+, NaChBac has a pore structure similar to that of voltage-gated Ca^{2+} channels (Durell and Guy, 2001; Ren et al., 2001; Yue et al., 2002). Third, NaChBac pharmacology resembles that of Ca^{2+} channels rather than that of Na^+ channels, being sensitive to block by divalent cations and agents like Nifedipine, and mostly insensitive to tetrodotoxin (Ren et al., 2001). Finally, NaChBac Na^+ current kinetics, including activation, inactivation, and recovery from inactivation are 10–100

Address correspondence to Ana M. Correa, Department of Anesthesiology, David Geffen School of Medicine at University of California, Los Angeles, BH-509A, CHS Box 957115, Los Angeles, CA 90095-7115. Fax: (310) 794-9612; email: nani@ucla.edu

A. Kuzmenkin was on leave from the Department of Applied Physiology, University of Ulm, D-89069 Ulm, Germany, his current address.

Abbreviations used in this paper: HP, holding potential; MS, methane sulfonate; NMG, *N*-methyl-D-glucamine.

times slower, compared with other voltage-gated Na^+ channels (Ren et al., 2001; Koishi et al., 2004).

As has been shown for K_VAP (Jiang et al., 2003), a potassium channel from the archeabacteria *Aeropyrum pernix*, one of the promising aspects of working with these prokaryotic channels is the feasibility of obtaining crystal structures that allow direct association of functional channel properties to its structural features. With the imminence of a crystal structure of NaChBac becoming available soon, it is desirable to have a detailed functional picture of NaChBac gating at macroscopic and molecular levels. In the present study, we recorded NaChBac gating and ionic currents from wild-type NaChBac expressed in mammalian COS-1 cells, applying the whole-cell patch-clamp technique. The results obtained from the analysis of nonsteady state and steady-state properties and from modeling of ionic currents at various voltages indicate that, similar to that of other voltage-gated Na^+ and K^+ channels, the activation pathway of NaChBac involves transitions between several closed states, leading to an open state and subsequent inactivated state.

MATERIALS AND METHODS

Molecular and Cell Biology

The cDNA for the wild-type NaChBac, in a modified pTracer-CMV2 expression vector was a gift of D. Ren (University of Pennsylvania, Philadelphia, PA) and D. Clapham (Harvard University, Boston, MA). The cDNA was amplified in bacterial culture and purified with QIAfilter™ Plasmid Maxi Kit (QIAGEN).

COS-1 cells (American Type Culture Collection) were transiently transfected with NaChBac cDNA using the commercial LipofectAMINE™ 2000 Reagent (Invitrogen) to deliver the pTracer expression clones. Standard procedures were followed for growth and maintenance of cells in culture. Transfected cells were identified by eGFP fluorescence encoded in the pTracer vector Cis to the NaChBac sequence. Patch-clamp recordings were done 48–72 h post-transfection.

Electrophysiology

Standard whole-cell recording methods were used as previously described (Hamill et al., 1981). The pulse protocols are described in RESULTS and in the figure legends. Linear capacitive currents and leak were subtracted using the P/−4 protocol (Bezanilla and Armstrong, 1977), whereby four subtracting pulses 1/4 the amplitude of the test pulse waveform but in the opposite direction were delivered immediately after the test pulse; the resulting currents were then averaged, scaled, and subtracted from the records. The time between subtracting pulses was 100 ms for current recovery. Subtracting holding potentials (HPs) were always equal to the HPs, usually −120 mV. The long interpulse interval (cycle period was 12 s for 10-ms pulses and 15 s for pulses up to 500 ms), the negative HP and subtracting region (−120 mV and less), and working at high temperature (28°C) all contribute to avoid current rundown and to maximize charge recovery. Capacitive transients were obtained for each experiment; the time needed to charge the cell membrane was always negligible compared with gating and ionic current kinetics (not depicted). Series resistance (Rs) was compensated in ionic current experiments using the voltage-clamp Rs circuitry; Rs errors were <4 mV. Data were filtered at 10 kHz and acquired using a custom-made program (GPatch). Pipette resistances were in the range 0.8–1.5 MΩ. Patch electrodes contained (in mM) 145 *N*-methyl-D-glucamine (NMG)-F, 5 choline-Cl, 5 EGTA-NMG, 10 HEPES-NMG, pH 7.4. The bath contained 140 NMG-methane sulfonate (MS), 0.5 $CaCl_2$, 10 $MgCl_2$, 10 HEPES-NMG, pH 7.4, for gating current experiments, or 105 NMG-MS, 35 NaCl, 0.5 $CaCl_2$, 10 $MgCl_2$, 10 HEPES-NMG, pH 7.4, for ionic current recordings. In a few experiments, the Na^+ bath concentration was decreased to 14 NaCl/126 NMG-MS (1/10 of full Na^+) to be able to detect gating and ionic current in the same cell. Corrections were made for liquid junction potentials. All experiments were performed at 28°C using a custom-made temperature controller except for Cole-Moore shift experiments, which were done at room temperature (19–21°C). At 28°C, channels activate and inactivate faster, thus, gating currents are easier to detect; also, ionic current amplitude is increased and recovery from inactivation is complete, pulsing every 12 to 15 s (Correa, 2004). Whole-cell data were analyzed with our in-house program (Analysis) and with the programs ORIGIN (OriginLab Corp.) and Excel (Microsoft Corp.). Data are presented as mean ± SEM. Student's *t* test was applied for statistical evaluation; the significance level was set at $P < 0.05$.

Estimation of Charges Per Channel

The charge per channel values (z) were estimated using the Q/N method, $z = Q/N$, where Q is the total charge translocated in response to a depolarizing step, taken as the maximal charge obtained from the charge versus voltage (Q–V) curves, and N is the number of channels in the cell. The charge at any given voltage V was determined from the time integral of the charge moved during the pulse. N was calculated from

$$N = \frac{\hat{I}_V}{i_V p_V^o},$$

where $\hat{I}_V$ is the amplitude of the ionic current elicited by depolarizing pulse of voltage V, long enough to reach the maximum, i_V is the single channel current, and p_V^o is the open probability at the same voltage. Single channel currents i_V at various potentials were estimated using data from single channel recordings in full sodium (140 mM) reported by Ren et al. (2001). These values were used to estimate i_V at 14 and 35 mM $[Na]_o$ (γ_o = 1.4 pS and 3.5 pS). Open probability values p_V^o were determined using data from ionic current experiments (this study), single channel currents, and ensemble current at −10 mV from Ren et al. (2001), as well as data from temperature-dependent changes in NaChBac gating (Correa, 2004).

Kinetic Simulation

For kinetic simulation of macroscopic ionic currents, we fitted sodium currents simultaneously at different voltages to the simplified sequential kinetic model presented in Fig. 5 A in RESULTS. The voltage-dependent forward and backward transition rates between various states were assumed to be single exponential functions of voltage (Stevens, 1978) and are given by

$$\alpha_1(V) = \alpha_1' \exp\left(\frac{z_1 x_1 FV}{RT}\right), \quad (1)$$

$$\beta_1(V) = \beta_1' \exp\left(\frac{-z_1(1-x_1)FV}{RT}\right)$$

for the activation and by

$$\alpha_2(V) = \alpha'_2 \exp\left(\frac{z_2 x_2 FV}{RT}\right), \quad (2)$$

$$\beta_2(V) = \beta'_2 \exp\left(\frac{-z_2(1-x_2)FV}{RT}\right)$$

for inactivation. The fitted parameters were: α'_1, β'_1, α'_2, and β'_2, the transition rate constants including enthalpic and entropic factors; z_1 and z_2, the valences of forward and backward transitions; x_1 and x_2, the fraction of the electric field where the barrier peak was located; V, the membrane potential; F, the Faraday constant; R, the gas constant; and T, the absolute temperature. The fit was performed with ScoP (Simulation Control Program) from Simulation Resources Inc.

RESULTS

NaChBac Gating Current Characteristics

NaChBac has activation and inactivation kinetics drastically slower than that of other voltage-gated sodium channels (Koishi et al., 2004). COS-1 cells, like COS-7 cells (Ren et al., 2001), express NaChBac very efficiently, often yielding several nanoamperes of ionic current. However, the gating currents are practically undetectable at room temperature because of the characteristic slow kinetics of the channel. To circumvent this problem, recordings were done at 28°C to accelerate the gating current kinetics, increase current amplitudes, and improve current recovery from inactivation (Correa, 2004). At this temperature, however, ionic currents are accelerated as well and contaminated gating current records. Even in Na^+-free bath solutions, the gating currents recorded in 1.5 mM Ca^{2+} were significantly contaminated by inward Ca^{2+} currents (unpublished data), presumably through NaChBac itself since it is slightly permeable to Ca^{2+} (Ren et al., 2001). To decrease ionic current contamination, the extracellular Ca^{2+} was reduced to 0.5 mM and 10 mM Mg^{2+} was added to maintain cell integrity.

In Fig. 1 A are original gating current traces elicited by a family of 10-ms depolarizing pulses from an HP of −150 mV to the indicated voltages. Gating currents became clearly detectable at −90 mV, and they increased and became faster with increasing depolarization. The magnitude of the charge moved upon depolarization ($I_{g\ ON}$) was comparable to that moved upon return to the HP ($I_{g\ OFF}$) for most potentials tested, especially in the nonlinear region of the Q–V curves (unpublished data), indicating that little, if any, charge immobilization occurred within the brief, 10-ms depolarizing period. For longer pulses, however, ionic tail currents, although small, contaminated $I_{g\ OFF}$, hindering accurate determinations of charge immobilization upon establishment of inactivation during the pulse. To address the question of charge immobilization by prolonged depolarization, the effect of the HP on the gating charge movement was assessed by recording gating currents

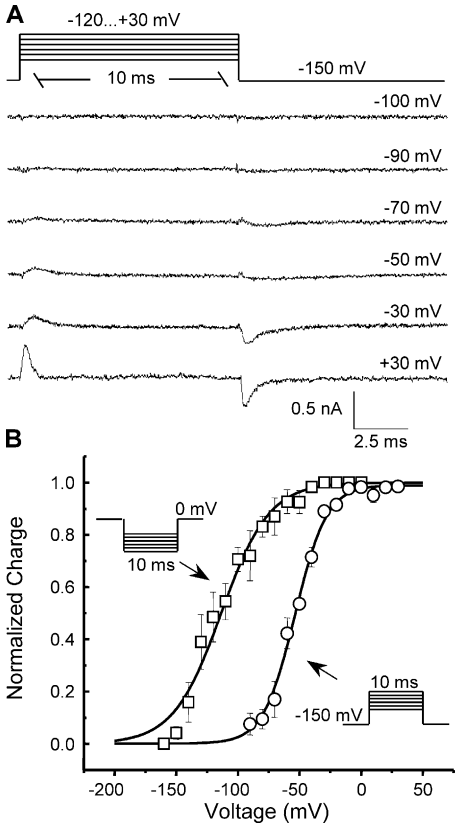

FIGURE 1. NaChBac gating current characteristics. (A) Original gating current traces elicited by a family of 10-ms depolarizations from a −150 mV HP to voltages ranging from −120 to 30 mV in 10-mV steps. Typical traces for several test pulse potentials are shown. (B) Charge–voltage (Q–V) relationship (open circles) from an HP of −150 mV, compared with Q–V from an HP of 0 mV (open squares). Curves are the fits to single Boltzmann functions of the form: $I(V) = A2 + (A1 - A2)/(1 + \exp(-(V - V_{1/2})/k))$, where $A1$ and $A2$ are amplitudes, V is the voltage, $V_{1/2}$ is the half-maximal voltage, and k is the slope factor. The fitted parameters were: $V_{1/2} = -54 \pm 2$ mV, $k = 12.3 \pm 1.6$, $n = 4$ (HP = −150 mV) *vs.* $V_{1/2} = -113 \pm 5$ mV, $k = 19.1 \pm 3.3$, $n = 3$ (HP = 0 mV), where n is the number of cells.

elicited by 10-ms pulses from an HP of 0 mV to voltages ranging from −160 mV to −10 mV in 10-mV steps. The corresponding Q–V curve, while exhibiting similar steepness ($P > 0.1$) to that of the control curve, was shifted by 59 mV to more negative potentials ($P < 0.0001$) relative to the Q–V from an HP of −150 mV (Fig. 1 B), suggesting that charge was immobilized by the prolonged depolarization (Bezanilla et al., 1982).

Sodium Current Measurements

To better characterize the NaChBac gating pathway and correlate macroscopic current kinetics with gating currents, sodium currents, I_{Na} (Fig. 2 A), were recorded using the same protocol used to elicit gating currents. The time to peak during 10-ms pulses was similar to or less than the depolarization time for most voltages

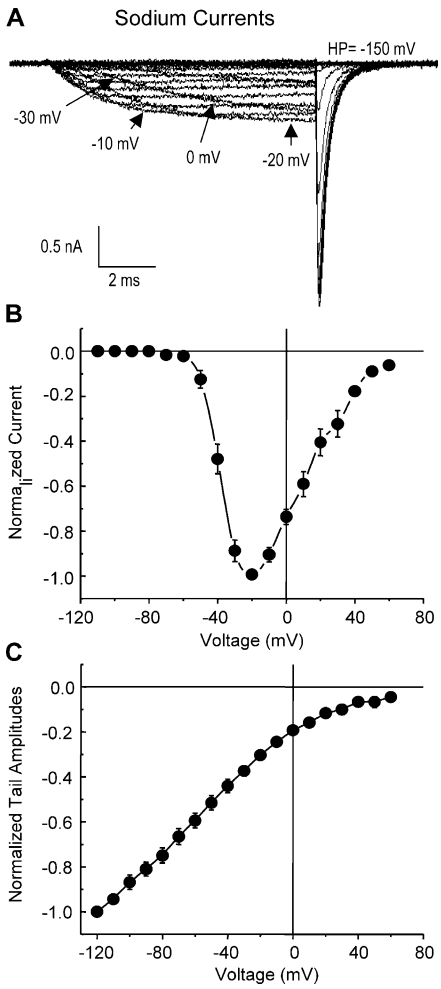

FIGURE 2. NaChBac ionic current characteristics. (A) Representative I_{Na} traces elicited by a family of 10-ms depolarizations from a −150-mV HP to voltages ranging from −120 to 80 mV in 10-mV steps. (B) Normalized current–voltage (I–V) relationships. Data were fit to a sigmoid function with $V_{1/2} = -36 \pm 1$ mV and $k = -5.6 \pm 0.1$, $n = 4$. (C) Instantaneous I–V curve obtained from normalized tail current amplitudes ($n = 5$) at the voltages plotted, following a 10-ms prepulse to −10 mV. HP was −120 mV.

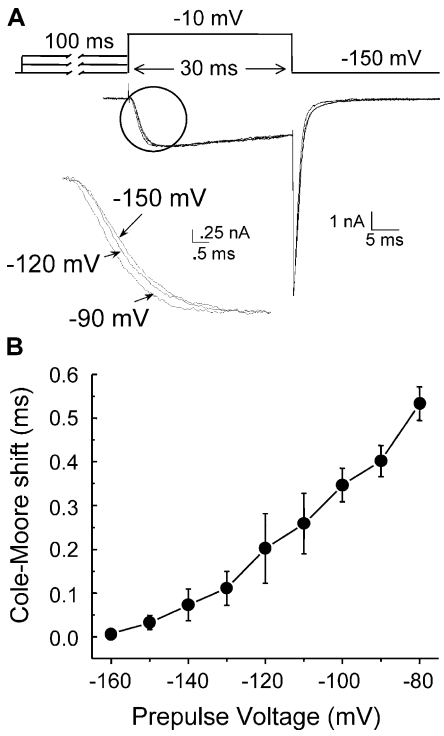

FIGURE 3. Cole-Moore shift. (A) I_{Na} traces elicited by a test pulse to −10 mV following a 100-ms preconditioning pulse to various potentials. For better resolution, recordings were done at the room temperature (∼21°C). HP was −150 mV. The circle indicates the region with expanded time resolution shown below. (B) Time shift to the half-maximal ionic current for indicated voltages ($n = 5$).

tested, except at very negative potentials, so that the constructed I–V curve (Fig. 2 B) resembles that obtained by longer depolarizations (not depicted). The average current versus voltage (I–V) curve shown in Fig. 2 B, constructed from individually normalized I–V curves, demonstrates that the ionic currents developed at more depolarized voltages than the I_g. I_{Na} elicited from an HP of −150 mV became visible at −75 mV and peaked at −20 mV. The instantaneous I–V curve for NaChBac (Fig. 2 C) was linear in the negative range of potentials but deviated at positive potentials, as expected from the absence of Na^+ in the pipette solution.

The conductance versus voltage relation (G–V) curve was estimated from peak tail current amplitudes at −150 mV after a 10-ms pulse to a voltage V. Interestingly, the relative position of a G–V curve in the voltage axis was found to be dependent on the length of the applied depolarizing test pulse. Nonetheless, the G–V curve obtained by interrupting a depolarizing pulse at the peak of the ionic current resembled that obtained using tail currents at −150 mV after a 10-ms pulse (unpublished data). In either case, the conductance of NaChBac was a sigmoidal function of voltage, developing positive to −80 mV with a maximum at ∼30 mV and a midpoint of activation close to −30 mV ($n = 5$; Fig. 4 A).

Cole-Moore Shift

I_{Na} develops with a brief lag of several microseconds upon depolarization. To determine whether the channel visits several closed states before opening, we applied the classical Cole-Moore protocol (Cole and Moore, 1960). The cell membrane was hyperpolarized to various potentials for 100 ms and, immediately thereafter, I_{Na} was tested with a short depolarizing pulse to −10 mV. In this case, experiments were done at 21°C to increase time resolution. Current traces for various potentials from the same cell were then scaled to the maximal ionic current (Fig. 3 A). We used the time shift from the start of the depolarizing pulse to the half-maximal ionic current as the value for the Cole-Moore shift

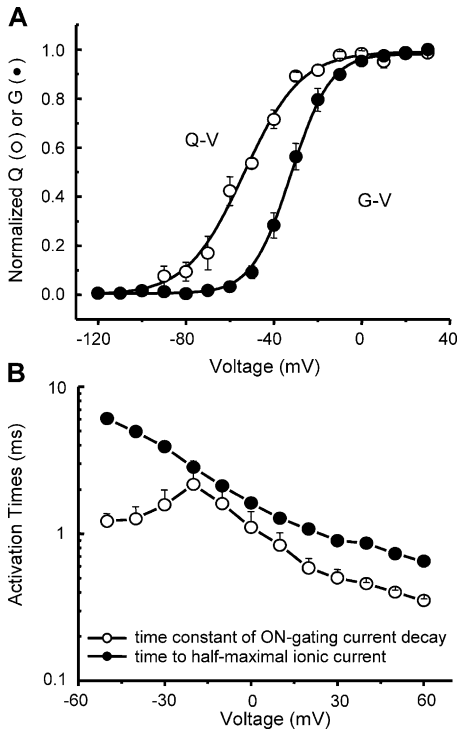

FIGURE 4. Charge movement and ionic conductance. (A) Q–V and G–V for an HP of −150 mV. Q–V is shifted by 22 mV toward more negative potentials and has less voltage dependence relative to the G–V. Both curves are the fits to Boltzmann functions with fit parameters: $V_{1/2} = -54 \pm 2$ mV, $k = 12.3 \pm 1.6$ (Q–V, $n = 4$) vs. $V_{1/2} = -32 \pm 2$ mV, $k = 8.0 \pm 0.4$ (G–V, $n = 5$), where $V_{1/2}$ is the midpoint potential of the curve, k is the slope factor, and n is the number of cells. (B) Single exponential time constants of $I_{g\ ON}$ decay ($n = 6$) and time to half-maximal ionic current as a function of voltage ($n = 4$).

(Fig. 3 B). The shift from −160 mV to −80 mV was 533 ± 38 μs ($n = 5$). No ionic current developed during the preconditioning pulse for any of the potentials plotted (Fig. 3 B). The observed Cole-Moore shift indicates that NaChBac goes through a series of closed states before channel opening. As the extent of the Cole-Moore shift is dependent on the preconditioning voltage, the population of these closed states is also voltage dependent, indicating charge movement between closed states.

The Relation Between Charge Movement and Ionic Conductance

When comparing NaChBac ionic and gating current steady-state curves, we observed that the Q–V curve was shifted by 22 mV to more negative potentials ($P < 0.0001$) and was less steep ($P < 0.03$) than the G–V curve (Fig. 4 A), suggesting that charge movement precedes channel opening, in complete agreement with the Cole-Moore shift results (see above). Times to half-maximal ionic current (activation half-times) and single exponential time constants of $I_{g\ ON}$ decay revealed similar dependence on voltage (Fig. 4 B), which suggests that the events are correlated.

TABLE I

Estimation of Charges Per Channel

Cell	1	2	3	4	5
Q, fC	134	131	150	97.8	66
N	47,332	45,126	65,529	43,264	34,741
$Z = Q/N$	17.8	18.2	16.2	14.3	12.6

Q, maximal amount of charge translocated in response to a depolarization; *N*, number of channels; *z*, calculated charge per channel (e_0).

Estimation of Charge Per Channel

To determine how many elementary charges in a single channel are translocated in response to membrane depolarization, in a separate set of experiments, we estimated the charge-per-channel values by measuring ionic currents and gating currents in the same cell. Table I represents the variation of these values among the cells tested. The mean value of elementary charges (e_0) per channel was 15.8 ± 1.2 e_0 ($n = 5$), which is higher than, but correlates well with, similar determinations in other voltage-gated channels (Schoppa et al., 1992; Aggarwal and MacKinnon, 1996; Noceti et al., 1996; Seoh et al., 1996).

Kinetics of NaChBac Gating

Further analysis of NaChBac gating kinetics was done fitting I_{Na} to the sequential state model presented in Fig. 5 A (Correa, 2004). To minimize the number of parameters, the model was made strictly sequential. Although this model clearly would not allow any detailed description of the recovery from inactivation process, the aim of this modeling was the prediction of the gating currents so they could be compared with the experimental data. I_{Na} traces elicited by 500 ms long depolarizing pulses to voltages in the range −40 mV to 0 mV in 10-mV steps were simultaneously fitted to the model. More negative potentials were not considered because of the relatively small ionic currents with very slow kinetics. Potentials >0 mV were excluded due to nonlinearity of the instantaneous I–V curves in this region (Fig. 2 C). Our fits suggest that the NaChBac gating can be well described by the model used (Fig. 5 B). The best-fit values were: $\alpha'_1 = 2.6 \pm 0.5\ ms^{-1}$, $\beta'_1 = 0.08 \pm 0.07\ ms^{-1}$, $\alpha'_2 = 0.034 \pm 0.005\ ms^{-1}$, $\beta'_2 = (2.8 \pm 1.4)*10^{-7}\ ms^{-1}$, $x_1 = 0.37 \pm 0.03$, $x_2 = 0.68 \pm 0.10$, $z_1 = 2.5 \pm 0.5\ e_0$, and $z_2 = 0.17 \pm 0.05\ e_0$; $n = 3$. Estimation of the backward transition rates β'_1 and β'_2 is less certain than that of the forward transition rates α'_1 and α'_2 because backward rates are much smaller than forward rates at the voltages fitted. However, the set of parameters found provides us with a fair description of NaChBac activation. Using the mean parameters obtained from the fits of ionic currents, we then simulated the NaChBac gating currents and fitted them to a single ex-

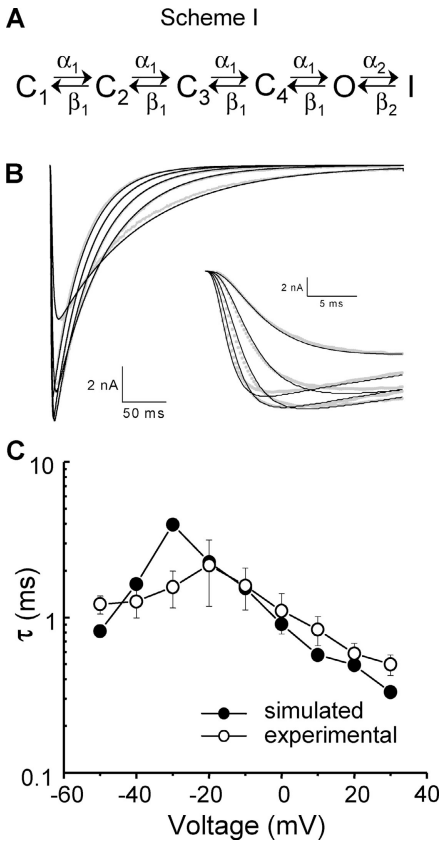

FIGURE 5. Kinetic simulations. (A) Sequential simplified model used for kinetic simulations. C_1–C_4 are four closed states, O is the open state, I is the inactivated state, and α_1, α_2, β_1, and β_2 are voltage-dependent transition rates between the states, as shown in the model. For simplicity, all transition rates in the activation pathway, C4 through O, were assumed to be equal. (B) Representative ionic current traces elicited by a family of 500-ms depolarizations from a −150-mV HP to voltages ranging from −40 to 0 mV in 10-mV steps, simultaneously fitted to the sequential model of NaChBac gating shown in A. Superimposed on the traces are the fitted curves. Inset, same as part B with expanded time scale. (C) Fit of predicted time course of gating currents compared with experimental data fits.

ponential function. The fitted time constants of the simulated gating currents corresponded well to the fitted time constants of experimental gating current traces (Fig. 5 C), suggesting that the experimentally recorded gating currents are indeed the result of charge movement that gives origin to the ionic currents of NaChBac.

DISCUSSION

NaChBac belongs to the family of voltage-gated ion channels that undergo transitions between several closed states preceding the open state. The energy landscape of the channel gating is altered with changes in the membrane potential, modifying the likelihood of the channels being in a particular state. As NaChBac is a member of the proposed new superfamily of voltage-gated bacterial sodium channels, NaBac (Koishi et al., 2004), with structure and features clearly distinct from other voltage-gated ion channels, it was of great interest to reveal the gating mechanism of this channel and to determine the structure–function relationships for it.

Gating currents of NaChBac have the conventional kinetics found in other voltage-dependent channels and reflect the charge movement through the electric field in response to changes in the membrane potential (Armstrong and Bezanilla, 1973; Schneider and Chandler, 1973; Keynes and Rojas, 1974). Q–V curves showed a standard sigmoidal dependence on voltage (Bezanilla, 2000). In this work, a closer look to the steady-state and kinetic parameters of NaChBac gating currents along with ionic current analysis has provided us with a more detailed picture of NaChBac operation.

Charge Immobilization Reflects a C-type Inactivation of NaChBac

The steady-state parameters of this channel show a large shift of the Q–V curve from HP of 0 mV to more hyperpolarizing potentials, compared with the Q–V dependence from HP of −150 mV. This phenomenon was originally described for the Na gating currents in squid axons (Bezanilla et al., 1982) and it was proposed that prolonged depolarization induces conformational changes of the protein so that the charge must follow a different, parallel pathway (Bezanilla et al., 1982; Olcese et al., 1997). In the case of NaChBac, the conformational changes leading to the leftward displacement of the Q–V curve may reflect C-type slow inactivation, as was shown for *Shaker* K^+ channels (Olcese et al., 1997) following similar protocols. Recent data from mutagenesis experiments reinforce this assumption (Pavlov et al., 2004). Slow inactivation has also been found to cause the shift of the Q–V curve to more negative potentials in Ca^{2+} channels (Shirokov et al., 1998).

Gating Pathway of NaChBac

The observed Cole-Moore shift (Cole and Moore, 1960) implies the presence of several closed states and voltage-dependent transitions between them (for review see Bezanilla, 2000). Charge movement between early closed states has been previously suggested to be the physical basis for the channels' voltage dependence as well as to give origin to the Cole-Moore shift (Taylor and Bezanilla, 1983; Stefani et al., 1994). Consistent with this finding, the voltage dependence of the translocated charge was significantly shifted to more hyperpolarizing potentials, compared with the conductance–voltage curve for NaChBac, demonstrating charge movement before channel opening. On the other hand, at potentials more positive than −10 mV, the charge saturates,

whereas the conductance is still increasing with voltage. This result indicates that a step leading into the open state carries less charge than the previous transitions. Consequently, it may become undetectable in the Q–V curve, while the conductance is still not maximal, since the channels only open when the last transition occurs. A similar process has been described in *Shaker* K^+ channels (Stefani et al., 1994). In fact, mutations in the S4 region of the *Shaker* channel have isolated the last step in the activation pathway by shifting its voltage dependence (Ledwell and Aldrich, 1999).

Additionally, it is very important to correlate the charge movement to the primary structure of NaChBac. This channel was reported to have a structure similar to that of other voltage-gated cation channels built up of six transmembrane segments, where the fourth transmembrane segment contains six positively charged amino acids (arginines), four of them in a regular arrangement, where two arginines are separated by two hydrophobic residues (Ren et al., 2001). This pattern has been proposed to entail the core of the voltage-sensing mechanism of voltage-gated cation channels (Noda et al., 1984; Stühmer et al., 1989; Yang and Horn, 1995; Aggarwal and MacKinnon, 1996; Seoh et al., 1996; Yang et al., 1996, 1997). Based on the NaChBac structure, we estimated the number of elementary charges moving in a single channel in response to membrane depolarization using a variant of the Q/N method (for different methods see Bezanilla, 2000). The analysis revealed 15.8 ± 1.2 e_0 per channel ($n = 5$), which is slightly higher than similar determinations for voltage-gated K^+ channels (between 12.3 e_0 and 13.6 e_0; Schoppa et al., 1992; Aggarwal and MacKinnon, 1996; Seoh et al., 1996), Na^+ channels (12 e_0; Hirschberg et al., 1995), and Ca^{2+} channels (9 e_0 using limiting slope, but 14–15 e_0 with mean variance analysis; Noceti et al., 1996). The difference found may be due to uncertainty in the estimation of N that could originate from the determination of the single channel current values used, which were estimated from the previous study by Ren et al. (2001), from differences in the solutions used, and from uncertainty in the actual value of the p_V^o at I_{peak} at high temperature. The error in the estimation of N from $\hat{I}_V$, p_V^o, and i_V could amount to 20–30%. As $\hat{I}_V$ is the experimentally determined peak current at each potential, the uncertainty in the value of $\hat{I}_V$ would be small. The uncertainty in the estimation of the real p_V^o at 28°C arises from insufficient data on the open probability at I_{peak} for each voltage, especially at potentials for which charge saturation occurs. A rough estimate of the p_V^o value at 28°C using data at −10 mV gave an increase in p_V^o of 7%. We have not measured the effect of temperature on the single channel conductance of NaChBac that would be important to determine i_V. However, the expected effect would be that of an increase of 1.2–1.3, similar to what has been found in other channels. Even so, if the channel has several open states, neither the Q/N method used here nor the limiting slope method (Almers, 1978; Sigg and Bezanilla, 1997) can be applied for the correct estimation (Horn, 1996; Noceti et al., 1996; Seoh et al., 1996; Sigg and Bezanilla, 1997; Bezanilla, 2000). Regardless of the uncertainties, the charge per channel found for NaChBac seems to lie within the range found in all six transmembrane segment voltage-gated cation channels where it has been measured.

Model of NaChBac Gating

For a more quantitative description of NaChBac gating, we examined the kinetic properties of sodium currents by fitting them simultaneously at different voltages to the sequential kinetic model proposed (Bezanilla et al., 1994). The important result is that the kinetics of gating currents predicted from ionic current experiments resembles the experimental data, implying that the gating currents are coupled to activation of NaChBac. The good fit of our data and the correlation between observed and predicted gating current kinetics indicate that this channel undergoes several transitions between closed states before the last step, which opens the channel. The Cole-Moore shift and the leftward shift of the Q–V curve compared with the G–V relation are also consistent with a multistate channel.

In conclusion, the results of this study indicate that NaChBac has several closed states with voltage-dependent transitions carrying charge movement between the states. The translocation of this gating charge causes activation of the channel.

We thank Dr. D. Ren and Dr. D. Clapham for their gift of NaChBac DNA in pTracer and Ms. Hongyan Guo for technical assistance.

This work was supported by National Institutes of Health GM-068044 (A.M. Correa) and GM-30376 (F. Bezanilla). A. Kuzmenkin was additionally supported by a German Research Foundation (DFG) Fellowship.

Lawrence G. Palmer served as editor.

Submitted: 30 June 2004
Accepted: 23 August 2004

REFERENCES

Aggarwal, S.K., and R. MacKinnon. 1996. Contribution of the S4 segment to gating charge in the *Shaker* K^+ channel. *Neuron.* 16: 1169–1177.

Almers, W. 1978. Gating currents and charge movements in excitatory membranes. *Rev. Physiol. Biochem. Pharmacol.* 82:96–190.

Armstrong, C.M., and F. Bezanilla. 1973. Currents related to movement of the gating particles of the sodium channels. *Nature.* 242: 459–461.

Bezanilla, F. 2000. The voltage sensor in voltage-dependent ion channels. *Physiol. Rev.* 80:555–592.

Bezanilla, F., and C.M. Armstrong. 1977. Inactivation of the sodium

channel. I. Sodium current experiments. *J. Gen. Physiol.* 70:549–566.

Bezanilla, F., R.E. Taylor, and J.M. Fernandez. 1982. Distribution and kinetics of membrane dielectric polarization. 1. Long-term inactivation of gating currents. *J. Gen. Physiol.* 79:21–40.

Bezanilla, F., E. Perozo, and E. Stefani. 1994. Gating of *Shaker* K^+ channels. II. The components of gating currents and a model of channel activation. *Biophys. J.* 66:1011–1021.

Cole, K.S., and J.W. Moore. 1960. Potassium ion current in the squid giant axon: dynamic characteristics. *Biophys. J.* 1:1–14.

Correa, A.M. 2004. Temperature modulation of NaChBac gating. *Biophys. J.* 86:114a (Abstr.).

Durell, S.R., and H.R. Guy. 2001. A putative prokaryote voltage-gated Ca^{2+} channel with only one 6TM motif per subunit. *Biochem. Biophys. Res. Commun.* 281:741–746.

Hamill, O.P., A. Marty, E. Neher, B. Sakmann, and F.J. Sigworth. 1981. Improved patch-clamp techniques for high-resolution current recording from cells and cell-free membrane patches. *Pflugers Arch.* 391:85–100.

Hirschberg, B., A. Rovner, M. Lieberman, and J. Patlak. 1995. Transfer of twelve charges is needed to open skeletal muscle Na^+ channels. *J. Gen. Physiol.* 106:1053–1068.

Horn, R. 1996. Counting charges. *J. Gen. Physiol.* 108:129–132.

Jiang, Y., A. Lee, J. Chen, V. Ruta, M. Cadene, B.T. Chait, and R. MacKinnon. 2003. X-ray structure of a voltage-dependent K^+ channel. *Nature.* 423:33–41.

Keynes, R.D., and E. Rojas. 1974. Kinetics and steady-state properties of the charged system controlling sodium conductance in the squid giant axon. *J. Physiol.* 239:393–434.

Koishi, R., H. Xu, D. Ren, B. Navarro, B.W. Spiller, Q. Shi, and D.E. Clapham. 2004. A superfamily of voltage-gated sodium channels in bacteria. *J. Biol. Chem.* 279:9532–9538.

Ledwell, J.L., and R.W. Aldrich. 1999. Mutations in the S4 region isolate the final voltage-dependent cooperative step in potassium channel activation. *J. Gen. Physiol.* 113(3):389–414.

Noceti, F., P. Baldelli, X. Wei, N. Qin, L. Toro, L. Birnbaumer, and E. Stefani. 1996. Effective gating charges per channel in voltage-dependent K^+ and Ca^{2+} channels. *J. Gen. Physiol.* 108:143–155.

Noda, M., S. Shimizu, T. Tanabe, T. Takai, T. Kayano, T. Ikeda, H. Takahashi, H. Nakayama, Y. Kanaoka, N. Minamino, et al. 1984. Primary structure of *Electrophorus electricus* sodium channel deduced from cDNA sequence. *Nature.* 312:121–127.

Olcese, R., R. Latorre, L. Toro, F. Bezanilla, and E. Stefani. 1997. Correlation between charge movement and ionic current during slow inactivation in *Shaker* K^+ channels. *J. Gen. Physiol.* 110:579–589.

Pavlov, E., C. Bladen, R.J. Winkfein, P.P.S. Dhaliwal, Q. Ma, and R.J. French. 2004. Inactivation in a bacterial voltage-gated sodium channel – a C-type mechanism? *Biophys. J.* 86:167a (Abstr.).

Ren, D., B. Navarro, H. Xu, L. Yue, Q. Shi, and D.E. Clapham. 2001. A prokaryotic voltage-gated sodium channel. *Science.* 294: 2372–2375.

Schneider, M.F., and W.K. Chandler. 1973. Voltage dependent charge movement of skeletal muscle: a possible step in excitation-contraction coupling. *Nature.* 242:244–246.

Schoppa, N.E., K. McCormack, M.A. Tanouye, and F.J. Sigworth. 1992. The size of gating charge in wild-type and mutant *Shaker* potassium channels. *Science.* 255:1712–1715.

Seoh, S.A., D. Sigg, D.M. Papazian, and F. Bezanilla. 1996. Voltage-sensing residues in the S2 and S4 segments of the *Shaker* K^+ channel. *Neuron.* 16:1159–1167.

Shirokov, R., G. Ferreira, J. Yi, and E. Rios. 1998. Inactivation of gating currents of L-type calcium channels. Specific role of the alpha 2 delta subunit. *J. Gen. Physiol.* 111:807–823.

Sigg, D., and F. Bezanilla. 1997. Total charge movement per channel. The relation between gating charge displacement and the voltage sensitivity of activation. *J. Gen. Physiol.* 109:27–39.

Stefani, E., L. Toro, E. Perozo, and F. Bezanilla. 1994. Gating of *Shaker* K^+ channels. I. Ionic and gating currents. *Biophys. J.* 66: 996–1010.

Stevens, C.F. 1978. Interactions between intrinsic membrane protein and electric field. An approach to studying nerve excitability. *Biophys. J.* 22:295–306.

Stühmer, W., F. Conti, H. Suzuki, X.D. Wang, M. Noda, N. Yahagi, H. Kubo, and S. Numa. 1989. Structural parts involved in activation and inactivation of the sodium channel. *Nature.* 339:597–603.

Taylor, R.E., and F. Bezanilla. 1983. Sodium and gating current time shifts resulting from changes in initial conditions. *J. Gen. Physiol.* 81:773–784.

Yang, N., and R. Horn. 1995. Evidence for voltage-dependent S4 movement in sodium channels. *Neuron.* 15:213–218.

Yang, N., A.L. George Jr., and R. Horn. 1996. Molecular basis of charge movement in voltage-gated sodium channels. *Neuron.* 16: 113–122.

Yang, N., A.L. George Jr., and R. Horn. 1997. Probing the outer vestibule of a sodium channel voltage sensor. *Biophys. J.* 73:2260–2268.

Yue, L., B. Navarro, D. Ren, A. Ramos, and D.E. Clapham. 2002. The cation selectivity filter of the bacterial sodium channel NaChBac. *J. Gen. Physiol.* 120:845–853.